Differential Inhibition of HIV-1 and SIV Envelope-Mediated Cell Fusion by C34 Peptides Derived from the C-Terminal Heptad Repeat of gp41 from Diverse Strains of HIV-1, HIV-2, and SIV

Elena Gustchina,[†] Gerhard Hummer,[†] Carole A. Bewley,*[,‡] and G. Marius Clore*[,†]

Laboratory of Chemical Physics, Building 5, National Institute of Diabetes and Digestive and Kidney Diseases, National Institutes of Health, Bethesda, Maryland 20892-0520, and Laboratory of Bioorganic Chemistry, Building 8, National Institute of Diabetes and Digestive and Kidney Diseases, National Institutes of Health, Bethesda, Maryland 20892-0820

Received November 30, 2004

The spectrum of inhibition of human (HIV) and simian (SIV) immunodeficiency virus envelope (Env)-mediated cell fusion by C34, a 34 residue peptide corresponding to the C-heptad repeat of gp41 (residues 628−661 of HIV-1 Env), has been examined using a panel of five envelope glycoproteins, three from HIV-1 (LAV, SF162 and 89.6) and two from SIV (mac239 and mac316), and six C34 peptides derived from three strains of HIV-1 (LAV, N CM, and O CM), two strains of HIV-2 (EHO and ALI), and one strain of SIV (African Green Monkey, AGM). A quantitative vaccinia-based reporter gene cell fusion assay was employed. The inhibition data from the panel of 30 C34/envelope glycoprotein combinations, which can be fit to a simple activity relationship with IC_{50} values spanning a range of over 4 orders of magnitude from 4 nM to 70 μM, permits one to rationalize both the potency and broadness of the inhibitory properties of the C34 peptides in terms of computed interaction free energies between the C34 peptides and the N-helical trimeric coiled-coil of gp41 and the helical propensities of the free C34 peptides. Of particular interest is the finding that the C34 peptide derived from the EHO strain of HIV-2 is a broad spectrum, highly potent inhibitor of Env-mediated cell fusion with IC_{50} values spanning a very narrow range from only 4 to 25 nM over the entire panel of HIV-1 and SIV envelope glycoproteins tested. This result suggests that C34 from HIV-2 EHO may present a potentially useful therapeutic agent against diverse and/or resistant strains of HIV-1.

Introduction

Human (HIV) and simian (SIV) immunodeficiency virus envelope (Env)-mediated cell fusion involves a series of events initiated by the binding of gp120 to CD4 and a chemokine coreceptor.[1−3] Following initiation, a pre-hairpin intermediate state of gp41 is formed in which the internal trimeric coiled coil of N-terminal helices (residues 542−591 of HIV-1 Env) is exposed and the N-terminal fusion peptide is inserted into the target membrane.[4−7] Ultimately, the formation of the fusogenic six-helix bundle of gp41 drives the apposition of the viral and target cell membranes and concomitant cell fusion occurs.[2,3] The structure of the fusogenic state of the gp41 ectodomain from HIV-1 and SIV has been solved by crystallography[8−11] and NMR,[12] and comprises an internal parallel trimeric coiled-coil of N-terminal helices surrounded by antiparallel C-terminal helices (residues 623−663 of HIV-1 Env). The pre-hairpin intermediate state of gp41 is the target for three classes of HIV Env-mediated cell fusion inhibitors that block the formation of the fusogenic six-helix bundle of gp41:[13] class 1 inhibitors bind to the exposed trimeric coiled-coil of N-helices,[13−19] class 2 bind to the exposed C-heptad repeat region,[13,20−24] and class 3 form heterotrimers of the N-terminal coiled-coil.[25] Inhibitors comprising peptides derived from the C-terminal helix of gp41 belong to the class 1 inhibitors.[14−16] One such compound, T20 (also known as DP178),[14] consisting of residues 638−673 of HIV-1 Env and extending 10 residues beyond the end of the C-terminal helix of the fusogenic form of gp41, has completed clinical trials and been approved by the FDA for the treatment of AIDS under the name enfuvirtide.[26−28] In cell fusion assays, however, a peptide known as C34 which comprises residues 628−661 of HIV-1 Env[15] and encompasses 83% of the C-terminal helix, has an IC_{50} of ∼5 nM against HIV-1 LAV and is about 10−20 times more potent than T20 in vitro.[19]

For inhibitors such as T20 or C34 to be maximally effective they need to display a broad spectrum of activity against a wide range of HIV strains. Resistance to T20 has already been observed.[27,28] In this paper we make use of a vaccinia-virus based reporter gene assay for Env-mediated cell fusion[29] to characterize the fusion inhibitory properties of C34 peptides derived from a variety of HIV-1, HIV-2, and SIV gp41's against envelope glycoproteins from diverse HIV-1 and SIV strains. We show that a C34 peptide derived from the EHO strain of HIV-2 is both highly potent over the complete spectrum of envelope glycoproteins and displays broad fusion inhibitory activity. The underlying basis for variations in C34 inhibitory properties is investigated both experimentally and by means of theoretical energy calculations.

* To whom correspondence should be addressed. G.M.C.: Tel (301) 496 0782, Fax (301) 496 0825; E-mail, mariusc@intra.niddk.nih.gov. C.A.B.: Tel (301) 594 5187; Fax (301) 402 0008; E-mail, caroleb@intra.niddk.nih.gov.
[†] Laboratory of Chemical Physics.
[‡] Laboratory of Bioorganic Chemistry.

10.1021/jm049026h
Published on Web 03/25/2005

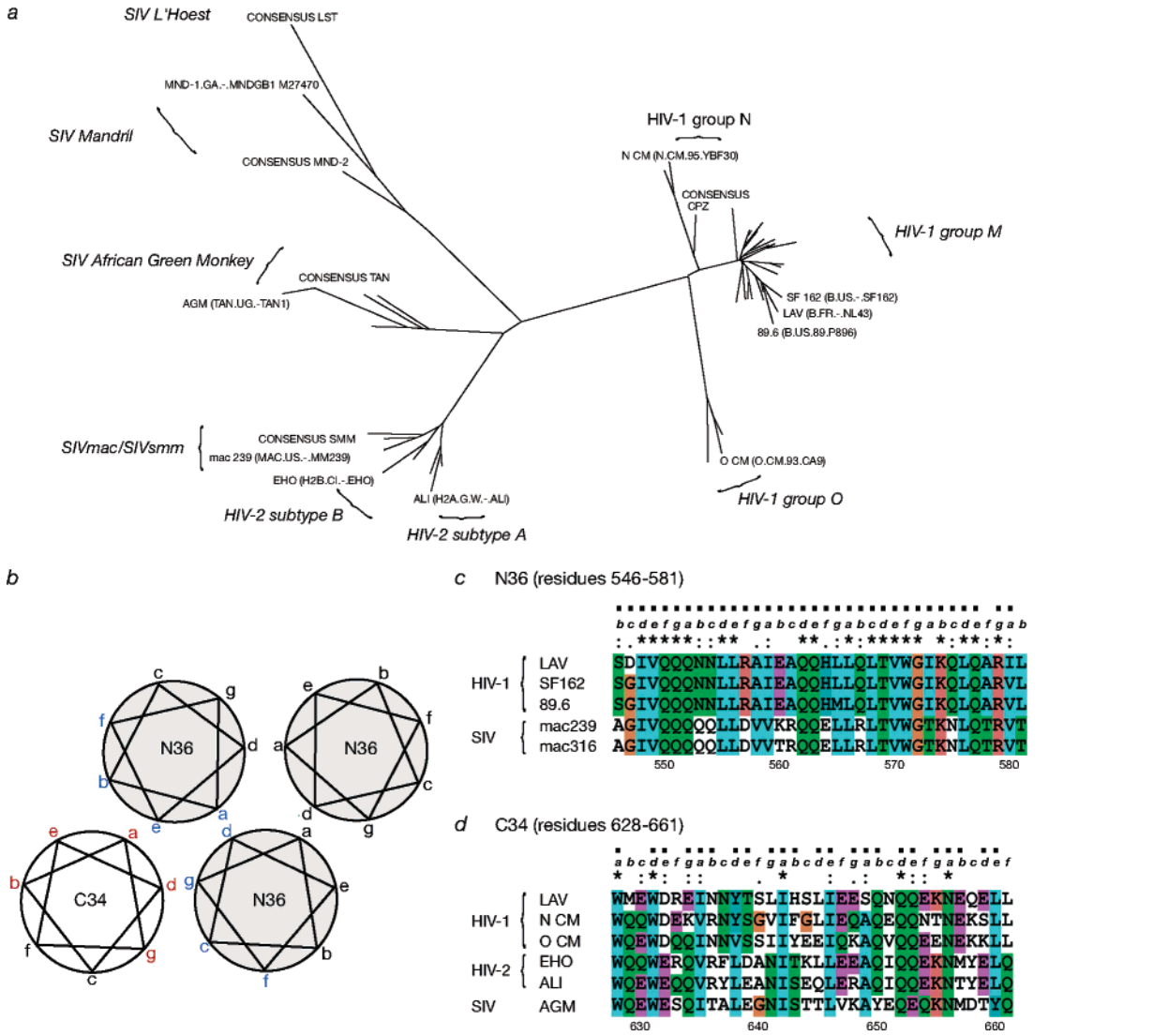

Figure 1. HIV-1 and SIV envelope glycoproteins and C34 peptides used to probe inhibition of HIV-1/SIV Env-mediated cell fusion. (a) Phylogenetic tree of HIV-1, HIV-2 and SIV derived from alignment of envelope glycoprotein (gp120/gp41) sequences. (b) Helical wheel representation depicting the interaction of the N- and C-heptad repeats observed in the three-dimensional structures of the fusogenic six helix bundle form of gp41.[8−12] The positions colored in blue for N36 (residues 546−581 in HIV-1 Env) and red for C34 (residues 628−661 in HIV-1 Env) correspond to sites involved in contacts between the two heptad repeats. Only a single C-helix is displayed. (c) Sequences of the N36 region of gp41 corresponding to the five envelope glycoproteins used in the current study, three from HIV-1 (LAV, SF-162 and 89.6) and two from SIV (mac239 and mac316). (d) Sequences of C34 peptides used in the current study, three from HIV-1 (LAV, N CM and O CM), two from HIV-2 (EHO and ALI) and one from SIV (AGM). In c and d, residues involved in contacts between the N- and C-helices in the six-helix bundle form of gp41 are indicated by solid squares; asterisks denote positions that are fully conserved; and colons and dots indicate positions in which one of the 'strong' (score > 0.5) or 'weaker' (score ≤ 0.5) positively scoring groups is conserved, respectively. The sequence alignments were generated using the program Clustal X 1.8 (ftp://ftp-igbmc.u-strasbg.fr/pub/ClustalX) operating in multiple alignment mode with the Gonnet Pam250 protein weight matrix.[40] Residues that are not conserved relative to the reference sequence (from HIV-1 HXB2) are uncolored, with the exception of glycine which is colored in orange whether it is conserved or not. Residues conserved relative to the reference HIV-1 HXB2 sequence are color coded as follows: nonpolar residues, blue; polar residues, green; aromatic polar residues, cyan; negatively charged residues, magenta; positively charged residues, red.

Experimental Section

gp41 Sequence Comparison. HIV-1, HIV-2, and SIV gp41 sequences were obtained from the HIV sequence database at Los Alamos National Laboratory (http://www.hiv.lanl.gov/content/hiv-db/mainpage.html). Sequence comparisons were performed using the ClustalX 1.8 sequence alignment program (ftp://ftpigbmc.ustrasbg.fr/pub/ClustalX/)

Peptides. All C34 peptides (Figure 1c), purchased from Biopeptide LLC (San Diego, CA), were synthesized on solid phase support, purified by reverse phase high performance liquid chromatography, and verified by mass spectrometry and quantitative amino acid analysis. All peptides bear an acetyl group at the N-terminus and an amide group at the C-terminus. Concentrations of peptides were determined spectrophotometrically, using molecular masses and extinction coefficients calculated with the ProtParam program (http://us.expasy.org/tools/protparam.html)

Circular Dichroism. CD spectra of peptides (at concentrations of 8−21 μg/mL) were recorded at 0 °C in 10 mM sodium phosphate buffer pH 7.5 on a JASCO J-720 spectropolarimeter using a 1 cm optical path length cell. Quantitative evaluation of secondary structure from the CD spectra was carried out using the program CDNN (http://www.bioinformatik.-biochemtech.uni-halle.de/cd_spect/index.html).[30]

Cell Fusion Assay. Inhibition of HIV/SIV Env-mediated cell fusion by the C34 peptides was carried out as described

previously[13] using a modification of the vaccinia virus-based reporter gene assay employing soluble CD4.[29]

B-SC-1 cells were used for both target and effector cell populations. For experiments employing Env from the T-tropic HIV-1 LAV strain, target cells were co-infected with recombinant vaccinia viruses vCB21R-LacZ (encoding β-galactosidase) and vCBYF1-fusin[31] (encoding CXCR4), and effector cells with vCB41[32] (encoding Env from HIV-1 LAV) and vP11T7gene1 (encoding T7 polymerase), at a multiplicity of infection (MOI) of about 2.5. In the experiments employing envelope glycoproteins from the M-tropic SF162 and dual-tropic 89.6 HIV-1 strains, as well as from the mac239 and mac316 strains of SIV, target cells were co-infected with vCB−CCR5[33] (encoding the CCR5 coreceptor) and vCB21R-LacZ, and effector cells with vCB32[32] (encoding Env from HIV-1 SF162), vBD3[34] (encoding Env from HIV-1 89.6), vCB74[35] (encoding Env from SIV mac239), or vCB75[35] (encoding Env from SIV mac316), and vP11T7gene1. Following infection for 1.5 h at 37 °C, cells were incubated for 18 h at 32 °C to allow for vaccinia virus-mediated expression of recombinant proteins.

For inhibition studies of Env-mediated cell fusion, peptides were added to an appropriate volume of DMEM 2.5% FCS and 10 mM phosphate buffer, pH 7.5 to yield identical buffer compositions (100 μL), followed by addition of 1×10^5 effector cells (in 50 μL of media) per well and 1×10^5 target cells (in 50 μL of media) per well. With the exception of experiments with Env from SIV mac316, recombinant soluble CD4 (Progenics Pharmaceuticals, Tarrytown, NY) was added to the media of the target cells at a concentration of 800 nM to yield a final concentration of 200 nM soluble CD4 per well. (This is double the concentration required to saturate the β-galactosidase signal[30]). In the case of the experiments employing Env from SIV mac316, however, no CD4 was employed since preliminary data indicated that the extent of fusion was essentially unaffected by the presence or absence of CD4. Following 2.5 h incubation at 37 °C, the assay plates were frozen overnight. β-Galactosidase activity of cell lysates was measured from the absorbance at 570 nm (Molecular Devices 96-well spectrophotometer) upon addition of chorophenol-red-β-D-galactopyranoside (Roche, Nutley, NJ). The curves for β-galactosidase activity versus C34 peptide inhibitor concentration were fit by nonlinear least-squares optimization using the program Kaleidagraph 3.5 (Synergy Software, Reading, PA).

Modeling and Interaction Free Energy Calculations. Interaction free energies for the binding of C34 peptides to the N-terminal helical coiled-coil of gp41 were estimated computationally using a molecular mechanics force field[36] with a generalized-Born (GB) model for solvent contributions to electrostatic interactions,[37] and a surface area (SA) model for hydrophobic interactions.[38] All calculations were performed using the Sander module of AMBER 8.0 (University of California at San Francisco). Initial structures for the six-helix bundle were built by homology modeling using the X-ray crystal structure (consisting of residues 546−581 and 628−661 of HIV-1 Env) with PDB code 1AIK[9] as a template. In the initial models, the backbone of the 1AIK structure was not changed, and the side-chain conformations of conserved amino acids were retained as well. Side-chains of amino acids that differed from those in 1AIK were modeled using the SCWRL 3.0 software.[39] In a few cases, the resulting side-chains had substantial steric overlap and were rebuilt using a second round of side-chain modeling with SCWRL. Glutamine headgroups with incorrect hydrogen-bonding geometry were rotated by 180°. The structural models included residues 548−581 (N-region) and 628−656 (C-region); that is, we only employed regions with complete overlap of the N- and C-helices within the 1AIK structure. The initial structures of the free C-peptides and of the trimeric N-peptide coiled coil were obtained by removing C-peptides from the six-helix bundle structure, leaving side chains and backbone intact. The resulting structures were energy minimized for 500 steps using a conjugate-gradient minimizer. From the resulting "free energies" (with solvent effects included through GB/SA terms) of the six-helix bundle (G_{N3C3}), the helical N-trimer (G_{N3}) and the helical C-peptide (G_C), we calculated the interaction free energy as $\Delta G_{inter} = G_{N3C3} - \{G_{N3} + 3G_C\}$. In this estimate, unfolding of C-peptide helices, as well as competing interactions in the dissociated state between the peptides and other parts of the protein, are neglected.

Table 1. Source of Envelope Glycoproteins Employed in the Current Study

strain	tropism	coreceptor
HIV-1 LAV	T tropic/CD4 dependent	CXCR4
HIV-1 SF162	M tropic/CD4 dependent	CCR5
HIV-1 89.6	Dual tropic/CD4 dependent	CCR5 or CXCR4
SIV mac239	T tropic/CD4 dependent	CCR5
SIV mac316	M tropic/CD4 independent	CCR5

Results and Discussion

Choice of Viral Envelope Glycoproteins and C34 Peptide Sequences. To assess as comprehensively as possible the fusion inhibitory activity of a range of different C34 peptides against envelope glycoproteins from a representative sample of HIV and SIV viruses, we initially constructed a phylogenetic tree based on the complete envelope glycoprotein (gp120/gp41) sequences (Figure 1a). Given the limited choice of available recombinant vaccinia virus strains expressing envelope glycoproteins, we selected envelope glycoproteins from three HIV-1 M group strains and two from SIVmac/SIVsmm strains (Table 1 and Figure 1c). The HIV-1 envelope glycoproteins employed originated from the T tropic X4 LAV-1, M tropic R5 SF162, and dual-tropic R5X4 89.6 strains of HIV-1. The two SIV envelope glycoproteins originated from T tropic/CD4 dependent mac239 and M tropic/CD4 independent mac316 strains of SIV.

The selection of C34 peptides was based on the following approach. HIV-1, HIV-2, and SIV gp41 sequences in the HIV DNA sequence database at Los Alamos National Laboratory were translated and compared using the Clustal X 1.8 package[40] operating in multiple alignment mode with the Gonnet Pam250 protein weight matrix. HIV-1 HXB2 was used as a reference strain for the purposes of residue numbering and selecting the appropriate region for alignment. After clustering sequences by organism and group (HIV-1), subtype (HIV-2), or species of origin (SIV), sequence "consensus" tables were generated in which sequences with relatively more conserved amino acids in common were clustered. This was used to derive common sequences for each lineage. Because of the large number of sequences and their variability, it was not feasible to take into account all of the substitutions within gp41 for further analysis. We therefore only considered the region from residues 546−581 (HIV-1 numbering) corresponding to the N-terminal helical coiled-coil of gp41 since the sequence variability within the C-heptad repeat region corresponding to C34 (residues 628−661) is much larger. The consensus sequences were then analyzed for substitutions in those residues involved in the primary (central) contacts between the N- and C-helical regions of gp41, namely positions ***e*** and ***g*** of the helical wheel in the case of the N-region and ***a*** and ***d*** in the case of the C-region (Figure 1b). Consensus sequences with the largest number of substitutions in these positions were selected and used to choose actual

Table 2. Percentage Sequence Identity within the N-Terminal Helical Region (residues 546−581 in HIV-1 Env) of gp41 among the Different Strains of HIV-1 and SIV Employed in the Current Study[a]

	% sequence identity				
	HIV-1			SIV	
	LAV	SF162	89.6	mac239	mac316
HIV-1 LAV	100	94	92	58	58
HIV-1 SF162	94	100	97	61	61
HIV-1 89.6	91	97	100	58	58
SIV mac239	56	65	62	100	97
SIV mac316	56	65	62	97	100

[a] The percentage sequence identities for all 36 residues is listed above the diagonal, and the percentage sequence identity for the 34 residues (see Figure 1b and c) that contact C34 is given below the diagonal.

Table 3. Percentage Sequence Identity for the C34 Peptides (corresponding to residues 628−661 of HIV-1 Env) Derived from the Various Strains of HIV-1, HIV-2 and SIV.

	% sequence identity					
	HIV-1			HIV-2		SIV
	LAV	N CM	O CM	EHO	ALI	AGM
HIV-1 LAV	100	47	53	44	38	24
HIV-1 N CM	57	100	50	44	38	27
HIV-1 O CM	57	57	100	35	44	32
HIV-2 EHO	52	52	44	100	79	44
HIV-2 ALI	44	48	44	78	100	50
SIV AGM	30	26	39	57	61	100

[a] The percentage sequence identities for all 34 residues is listed above the diagonal, and the percentage sequence identity for the 23 residues (see Figure 1b and d) that contact the N36 region of gp41 is given below the diagonal.

sequences from 'representative strains' from each group. The resulting panel of C34 peptide sequences is shown in Figure 1d. In the case of SIV, we chose a C34 sequence from the African Green Monkey (AGM) lineage since it had the largest number of amino acid substitutions in the positions of interest and the highest degree of divergence from the HIV-1 and HIV-2 lineages.

A comparison of the overall sequence identity for the N-region of gp41 (residues 546−581 of HIV-1 Env) and C34 peptides (residues 628−661 of HIV-1 Env) employed, as well as the sequence identity for residues involved in contacts between the N- and C-helical regions of gp41, is provided in Tables 2 and 3, respectively. In the case of the N-terminal helical coiled-coil of gp41 (Table 2), there is a high degree of sequence conservation (>90%) between the three HIV-1 strains and between the two SIV strains, but significantly less between the HIV-1 and SIV strains (ca. 55−65%). In comparison to the N-region, the degree of sequence conservation (both overall and for residues contacting the N-terminal helical coiled-coil) between the different C34 sequences is much less, ranging from 25 to 65% (Table 3).

C34 Peptide Inhibition of HIV/SIV Env-Mediated Cell Fusion. To ascertain the effect of sequence variation on C34 inhibition of HIV/SIV Env-mediated cell fusion, we carried out a quantitative vaccinia virus-based reporter gene cell fusion assay[13,30] for all 30 envelope glycoprotein/C34 peptide combinations. An example of the quality of the data is shown in Figure 2 which displays inhibition curves of Env-mediated cell fusion by C34 LAV with IC_{50}s spanning over 3 orders of magnitude ranging from 4.5 ± 1.0 nM against Env from HIV-1 LAV to 21 ± 2 μM against Env from SIV mac316. Note that all the data can be fit to a simple activity relationship of the form %fusion = 100/(1 + [C34]/IC_{50}) indicating that inhibition of fusion by the C34 peptides involves a single binding event (i.e. binding of only one molecule of C34 per molecule of gp41, in its pre-hairpin intermediate state, is all that is required to inhibit fusion).

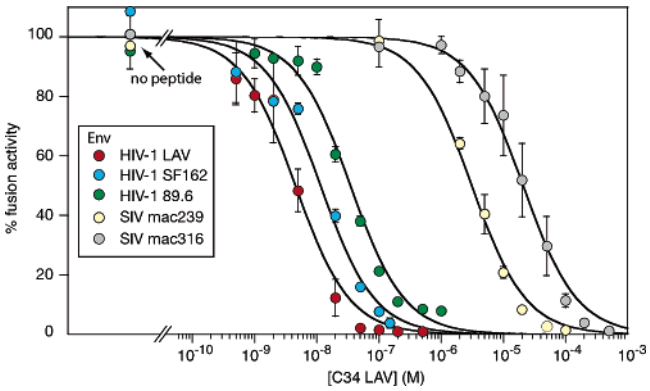

Figure 2. Inhibition of HIV-1 LAV, HIV-1 SF162, HIV-1 89.6, SIV mac239, and SIV mac316 Env-mediated cell fusion by the C34 peptide derived from HIV-1 LAV. The circles represent the experimental data; the vertical bars, the standard deviations for the experimental data; and the solid lines, the fits to the experimental data using the simple activity relationship: %fusion = 100/(1 + [C34]/IC_{50}).

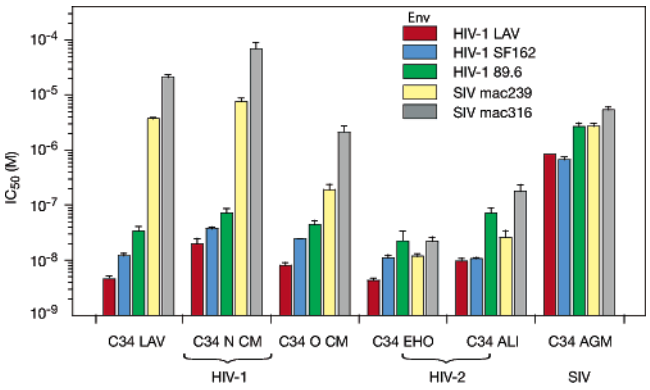

Figure 3. Summary of the IC_{50}s for inhibition of HIV-1/SIV Env-mediated cell fusion by C34 derived from three strains of HIV-1 (LAV, N CM, and O CM), two strains of HIV-1 (EHO and ALI), and one strain of SIV (AGM, African green monkey). Each C34 peptide was tested in the cell−cell fusion assay against five different envelope glycoproteins, three from HIV-1 (LAV, SF162 and 89.6) and two from SIV (mac239 and mac316).

A summary of all the IC_{50} data is provided in Figure 3 and Table 4. In the case of all six C34 peptides a general trend emerges in which inhibition of Env-mediated cell fusion decreases in the order HIV-1 LAV, HIV-1 SF162, HIV-1 89.6, SIVmac239, and SIVmac316 envelope glycoproteins. However, there is a large variation in the spectrum of inhibition with IC_{50}s ranging over 3 orders of magnitude for C34 from HIV-1 LAV and N CM, to less than an order of magnitude for C34 from HIV-2 EHO and SIV AGM. Of the six C34 peptides, C34 derived from the EHO strain of HIV-2 is both the most potent and has the broadest spectrum with an IC_{50} ranging from 4.3 ± 0.4 nM against Env from HIV-1 LAV to 20−25 nM against Env from HIV-1 89.6 and SIV-mac316. This result suggests that C34 derived from the HIV-2 EHO strain may be advantageous in terms of

Table 4. Inhibition (IC_{50}) of HIV/SIV Env-Mediated Cell Fusion by C34 Peptides Derived from HIV-1, HIV-2, and SIV

	envelope glycoprotein IC_{50} (M)				
C34 peptide	HIV-1 LAV	HIV-1 SF162	HIV-1 89.6	SIV mac239	SIV mac316
C34 HIV-1 LAV	$4.5(\pm1.0) \times 10^{-9}$	$1.2(\pm0.2) \times 10^{-8}$	$3.5(\pm0.3) \times 10^{-8}$	$3.1(\pm0.3) \times 10^{-6}$	$2.1(\pm0.2) \times 10^{-5}$
C34 HIV-1 N CM	$2.0(\pm0.5) \times 10^{-8}$	$3.8(\pm0.2) \times 10^{-8}$	$7.2(\pm1.5) \times 10^{-8}$	$7.7(\pm1.1) \times 10^{-6}$	$7.0(\pm2.1) \times 10^{-5}$
C34 HIV-1 O CM	$8.1(\pm0.9) \times 10^{-9}$	$2.5(\pm0.2) \times 10^{-8}$	$4.6(\pm1.3) \times 10^{-8}$	$1.9(\pm0.4) \times 10^{-7}$	$2.1(\pm0.6) \times 10^{-6}$
C34 HIV-2 EHO	$4.3(\pm0.4) \times 10^{-9}$	$1.1(\pm0.2) \times 10^{-8}$	$2.4(\pm1.2) \times 10^{-8}$	$1.2(\pm0.1) \times 10^{-8}$	$2.2(\pm0.4) \times 10^{-8}$
C34 HIV-2 ALI	$9.7(\pm1.1) \times 10^{-9}$	$1.1(\pm0.1) \times 10^{-8}$	$7.3(\pm1.7) \times 10^{-8}$	$2.6(\pm0.8) \times 10^{-8}$	$1.8(\pm0.5) \times 10^{-7}$
C34 SIV AGM	$8.4(\pm0.1) \times 10^{-7}$	$6.7(\pm0.8) \times 10^{-7}$	$2.7(\pm0.4) \times 10^{-6}$	$2.7(\pm0.3) \times 10^{-6}$	$5.4(\pm0.6) \times 10^{-6}$

therapeutic potential against diverse and/or resistant strains of HIV-1 and HIV-2.

Qualitative Structural Model-Based Rationalization of the Experimental IC_{50} Data. Models of the gp41 ectodomain core based on the crystal structure of the $(N36{\cdot}C34)_3$ six helix-bundle[9] were built as described in the Experimental Section. To some extent the general inhibition trend for the various C34 peptides (corresponding to residues 628−661 of HIV-1 Env) across the five different HIV-1/SIV envelope glycoproteins can be rationalized qualitatively, by reference to the helical wheel representation of the fusogenic form of the gp41 ectodomain shown in Figure 1b. The N36 region of HIV-1 LAV and SF162 differ at two positions (Figure 1c): D547G and I580V located at positions ***c*** and ***a***, respectively, of the helical wheel. The former entails the loss of an electrostatic interaction with Lys655 at position ***g***, while the latter substitution is neutral since it is not involved in any contact with C34. The L565M substitution (position ***g***) from SF162 to 89.6 HIV-1 (Figure 1c) may result in a reduction in hydrophobic packing with I642, Y/V/L638 and I/V635 (at positions ***a***, ***d***, and ***a***, respectively, Figure 1d). The single substitution between mac239 and mac316 SIV Env (Figure 1c), K650T (position ***b***), may result in a reduction in hydrophobic contacts with I/L646 (position ***e***; Figure 1d).

There are nine substitutions between the N36 region of HIV-1 89.6 and SIV mac239, of which six are involved in contacts with C34 (Figure 1c). Of these six substitutions, four may have untoward effects on binding affinity: N554Q (position ***c***) may generate a steric clash with Q652 (position ***d***) resulting in potential loss or weakening of a hydrogen bond; I573T (position ***a***) may reduce the packing with W631 (position ***d***) and W628 (position ***a***); Q575N (position ***c***) may result in the loss of a hydrogen bond with the side chain Nϵ atom of W628 (position ***a***); and finally L581T (position ***b***) may result in a reduction of hydrophobic contact with the indole ring of W628 (position ***a***). The remaining two substitutions are probably neutral owing to compensatory changes. Thus, Q567R (position ***b***) replaces a hydrogen bond between Q567 and T/S639 (position ***e***) with an alternate salt bridge between R567 and D/E639; likewise E560K (position ***b***) probably preserves an electrostatic interaction with Q/Y650 (position ***b***).

Semiquantitative Rationalization of the Experimental IC_{50} Data Based on Calculated Interaction Free Energies. A semiquantitative rationalization of the measured IC_{50} data can be derived from the results of energy minimization calculations using a generalized-Born model for solvent contributions to electrostatic interactions in conjunction with a surface area model for hydrophobic interactions (see Experimental for details). In this approach the energy and solvation free energy of the six-helix bundle N_3C_3 complex ($G_{N_3C_3}$), the

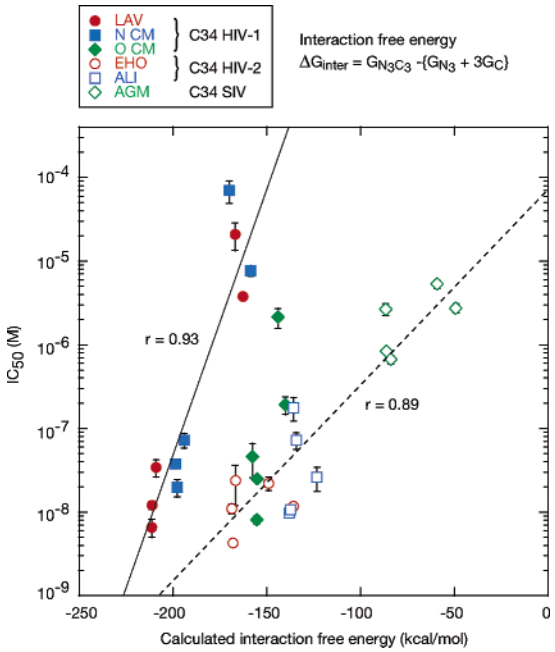

Figure 4. Correlation of the observed IC_{50}s versus the calculated interaction free energy. The data fall into two clusters: C34 from the LAV and N CM strains of HIV-1, and C34 from the HIV-1 O CM strain, the HIV-2 EHO and ALI strains, and the SIV AGM strain. The calculated interaction free energy (ΔG_{inter}) is given by $\Delta G_{inter} = G_{N_3C_3} - \{G_{N_3} + 3G_C\}$, where $G_{N_3C_3}$, G_{N_3}, and G_C are the computed free energies of the six-helix bundle, the isolated N-helical trimer, and the isolated C-helix, respectively.

N-helical trimer (G_{N_3}), and the isolated helical C34 (G_C) are computed, and an estimate of the interaction free energy is calculated as $\Delta G_{inter} = G_{N_3C_3} - \{G_{N_3} + 3G_C\}$. The results serve to highlight trends since unfolding of C-peptide helices, as well as competing interactions in the dissociated state between the peptides and other parts of the protein, are neglected. A plot of the experimental IC_{50}s versus the calculated interaction free energies is shown in Figure 4. In interpreting this plot several factors need to be borne in mind. First, since the number of data points per C34 peptide is limited to only five, correlations for individual C34 peptide datasets may not be apparent, and hence it is important to consider the data for several C34 peptides together. Second, the absolute values of the calculated interaction free energies, as is typical of molecular mechanics calculations, are not meaningful and the magnitude of the energetic differences appear to be too large (i.e. the slope in the logIC_{50} versus interaction free energy plot is too small). Third, energetic offsets between the different C34 datasets will reflect the properties of the free C34 peptides that were not taken into account in the calculations. When the data for all C34 peptides is considered as a whole, a trend between observed IC_{50}s

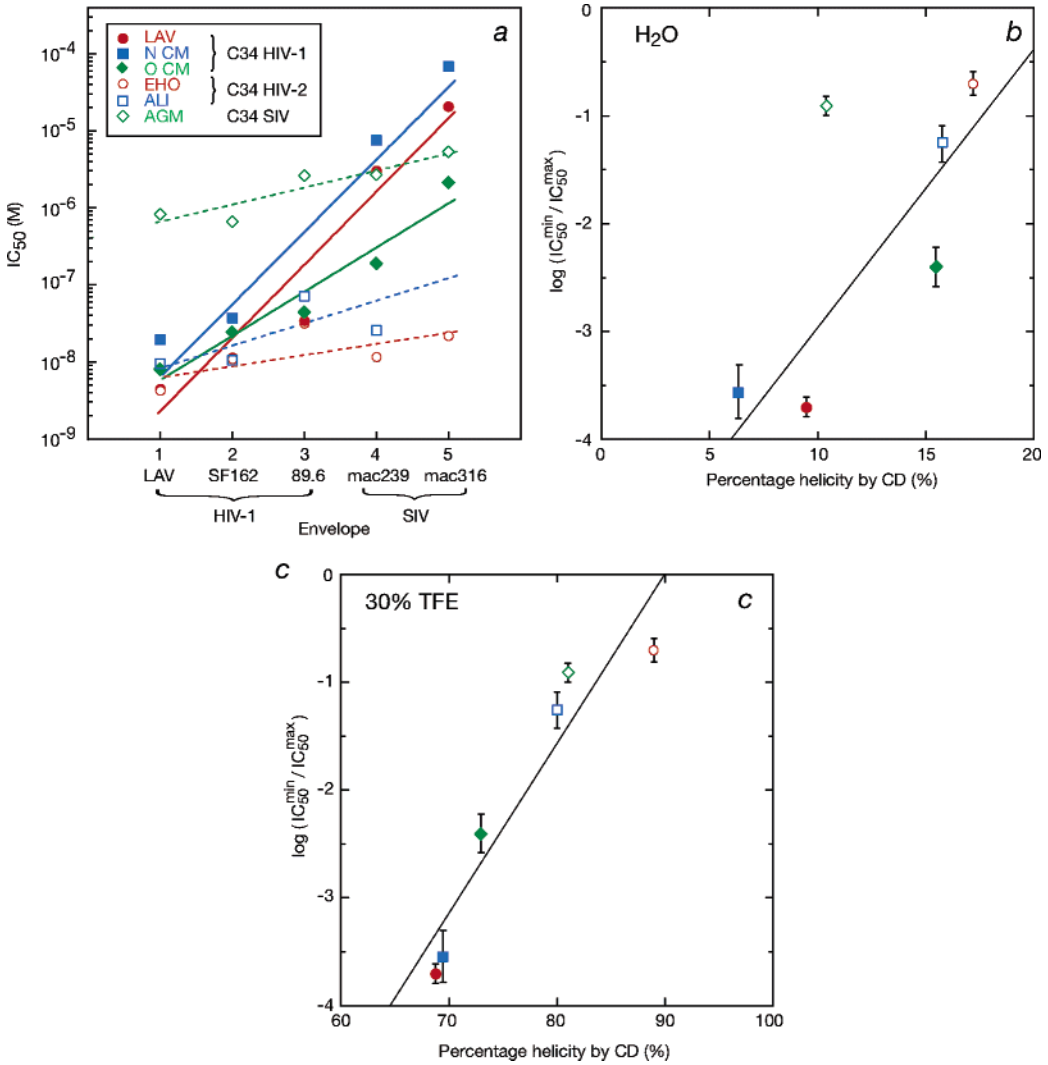

Figure 5. Broadness of the inhibition spectrum of HIV-1/SIV Env-mediated cell fusion by C34 peptides is correlated to their helical propensity. (a) Summary of the IC_{50} data for the various C34 peptides against a range of HIV-1 and SIV envelope glycoproteins. (b and c) Correlation of $\log(IC_{50}^{min}/IC_{50}^{max})$ versus percentage helicity determined experimentally by CD in water and 30% trifluoethanol, respectively. $\log(IC_{50}^{min}/IC_{50}^{max})$ (derived from linear regression analysis of the data shown in panel a) provides a measure of the broadness of the inhibition spectrum (i.e. the smaller the variation across the different envelope glycoproteins, the broader the inhibitory spectrum of a given C34 peptide). The correlation coefficient between $\log(IC_{50}^{min}/IC_{50}^{max})$ and helicity is 0.91 for the data in water (omitting the data point for C34 AGM) and 0.95 for the data in 30% trifluroethanol. (Note: trifluoroethanol promotes helical formation by effectively reducing the water activity of the solvent).

and calculated interaction free energies is apparent, but the correlation is rather poor (with a correlation coefficient of only 0.4). However, two sets of excellent correlations (each with a correlation coefficient of around 0.9) are observed: one for the C34 peptides from HIV-1 LAV and N CM, and the other for the C34 peptides from EHO and ALI HIV-2 and AGM SIV). The data for C34 from HIV-1 O CM also falls in the second group with the possible exception of a single data point, namely the IC_{50} for inhibition of SIV mac316 Env-mediated cell fusion. As will be shown in the following section, the presence of these two families can be accounted for by the helical propensities of the individual C34 peptides. This suggests that the folding stability of the free C34 peptides and other possible nonspecific interactions will be important for a fully quantitative description. Nevertheless, the global trends within the experimental data are reasonably well emulated by the theoretical calculations, particularly when taking into account inherent limitations of the modeling and molecular mechanics approach.

Correlation of Inhibition Spectrum with C34 Helical Propensity. The fusion inhibition data clearly show that the various C34 peptides exhibit differential ranges of IC_{50} against envelope glycoproteins from various strains of HIV-1 and SIV (Figures 3 and 5a). A measure of the broadness of the inhibition spectrum is provided by the logarithm of the ratio of the minimum to maximum IC_{50} value within a given C34 peptide series. Since the C34 peptides are dynamically disordered in aqueous solution, as judged by the absence of any chemical shift dispersion beyond that expected for a random coil in a one-dimensional ^1H NMR spectrum (unpublished observations), yet form six-helix bundles with the N-helical trimer of gp41, it is reasonable to postulate that the inhibition spectrum is related to some extent to the inherent helical propensity of the C34 peptides. This was not taken into consideration in the computed

interaction free energies. (The latter would be very difficult to do since it would require one to not only generate a realistic ensemble representation of the free C34 peptides but also to take into account potential nonspecific interactions, both of which are not feasible using current methodology,). The helical propensity, however, of the C34 peptides can be readily ascertained experimentally by CD spectroscopy. To this end CD spectra of the six C34 peptides were measured both in water and in 30% trifluoroethanol, a solvent known to promote helix formation by desolvation of hydrogen bond donors and acceptors.[41] The results are displayed in Figure 5b (for the data in water) and 5c (for the data in 30% trifluoroethanol) where a clear correlation is observed between $\log(IC_{50}^{min}/IC_{50}^{max})$ and percentage helicity. The correlation coefficient is 0.91 for the data in water omitting the data point for C34 AGM, and 0.95 for the data in 30% trifluoroethanol. It is also worth noting that there is an excellent correlation ($r = 0.94$) between the percentage helicity in water derived from the CD measurements and that predicted by the AGADIR prediction algorithm based on helix/coil transition theory.[42]

The C34 helix is amphipathic with an external hydrophilic face and a hydrophobic face that interacts with the internal trimeric coiled-coil of gp41. It therefore seems reasonable to anticipate that the helicity of the C34 peptides observed in 30% trifluoroethanol provides a better measure of helical propensity in the context of an interaction with the N-terminal coiled-coil of gp41 than that observed in water (i.e. the promotion of C34 helix formation by trifluoroethanol can be regarded as approximately analogous to that by the internal trimeric coiled-coil of gp41). This would account for the higher correlation of $\log(IC_{50}^{min}/IC_{50}^{max})$ with helicity in 30% trifluoroethanol (Figure 5c) than in water (Figure 5b).

It is also worth noting that the helical propensities of the C34 peptides in both water and 30% trifluoethanol fall into two major groups (Figure 5b and c): a low helical propensity group comprising C34 from HIV-1 LAV and N CM, and a high helical propensity group comprising C34 from HIV-2 EHO and ALI. C34 from SIV AGM falls in the high helical propensity group in trifluoroethanol, while C34 from HIV-1 O CM falls into the high helical propensity group in water and is of intermediate helical propensity in trifluoroethanol. These helical propensity groupings are in accord with the two sets of correlations observed in the plot of experimental IC_{50} versus calculated interaction free energy shown in Figure 5.

Concluding Remarks

We have examined the inhibition of HIV and SIV Env-mediated cell fusion by a series of C34 peptides derived from various strains of HIV-1, HIV-2, and SIV using a quantitative cell fusion assay. The data are accounted for by a simple activity relationship indicating that inhibition of cell fusion requires the binding of only a single molecule of C34 per molecule of gp41. Thus, one can conclude that the inhibitory properties of the different C34 peptides are directly related to their affinity for the N-terminal trimeric coiled-coil region of membrane bound gp41 in its pre-hairpin intermediate state. This is consistent with a previous study in which it was shown that $\log IC_{50}$ measured for HIV-1 C34 containing a series of six substitutions at a single key site (Trp631), known from structural work[8−12] to interact with a hydrophobic groove on the surface of the trimeric coiled-coil of N-helices, is directly correlated to the T_m of the corresponding six-helix bundle formed by N36 (residues 546−581 of HIV-1) and C34 peptides.[15] (Note that the measured IC_{50}s spanned a relative narrow range from about 1 to 40 nM, while the T_m ranged from ∼35 to ∼65 °C.[15]). A correlation between $\log IC_{50}$ for three different C34 peptides (from HIV-1_{IIIB}, HIV-2_{SBL}, and SIV_{Mac251}) and the T_m for various N36/C34 complexes (in those cases where a stable complex could be prepared) has also been reported.[44] It should be borne in mind, however, that correlating IC_{50}s with the T_ms for N36/C34 complexes involving different N36 peptides is fraught with difficulty since the T_m of the six helix bundle is determined not only by the interaction of C34 with N36, but also by the interaction between the N36 peptides themselves which form the internal trimeric coiled-coil around which the C34 peptides are wrapped.

The data reported here indicate that the spectrum of inhibition is significantly different for the diverse C34 peptides. With the exception of C34 derived from SIV AGM, all the HIV-1- and HIV-2-derived C34 peptides are approximately equipotent against envelope glycoproteins from HIV-1 LAV, SF162, and 89.6 with IC_{50}s ranging from 4 to 20, 10−40, and 30−70 nM, respectively (Figure 3). The range of inhibitory activity against envelope glycoproteins from SIV mac239 and mac316, however, is much larger ranging from 10 nM to 8 μM and from 20 nM to 70 μM, respectively (Figure 3). Of particular note is that the span of IC_{50}s observed for the HIV-2- and SIV-derived C34 peptides is around an order of magnitude compared to 2−3 orders of magnitude for the HIV-1-derived C34 peptides (Figure 3). The span of IC_{50}s over the diverse panel of HIV-1 and SIV envelope glycoproteins is a measure of the broadness of the inhibition spectrum. Thus, HIV-2- and SIV-derived C34 peptides are broad spectrum inhibitors whereas HIV-1-derived C34 peptides display a far narrower spectrum of inhibition (Figures 3 and 5a). Experimentally, this correlates with the helical propensity of the C34 peptides (Figure 5b and c). This is consistent with previously published data on constrained peptide analogues of T20 (residues 643−678 of HIV-1 Env) which demonstrated that increased potency against a single HIV-1 strain can be achieved by engineering an intramolecular disulfide bridge to increase the helical content of the free peptide.[43]

The results obtained with C34 derived from the HIV-2 EHO strain are of particular interest and practical significance since this particular C34 peptide displays both very high potency and broad spectrum inhibitory properties (with IC_{50}s spanning a narrow range from only 4 to 25 nM over all the tested HIV-1 and SIV envelope glycoproteins; Figure 3), suggesting that it may represent a potentially valuable therapeutic agent. It has previously been suggested, based on a much smaller panel of C34 peptides, that inhibition of HIV-2/SIV Env-mediated cell fusion is more difficult than HIV-1 Env-mediated cell fusion because CD4 destabilizes HIV-1 Env to a greater degree than HIV-2/SIV Env, thereby exposing the N-terminal helical coiled-coil for a longer period of time.[44] This longer exposure is presumed to

increase the time during which inhibitors can target the pre-hairpin intermediate state of gp41. The inhibition data with the C34 peptide from HIV-2 EHO, which is essentially an equipotent inhibitor of both HIV-1 and SIV Env-mediated cell fusion, indicates that differential destabilization of the various envelope glycoproteins by CD4 does not appear to be a major determinant of the fusion inhibitory properties of C34 peptides. Indeed, inhibition of SIVmac316 Env-mediated cell fusion by the C34 EHO peptide is highly effective despite the fact that fusion by SIVmac316 Env is essentially CD4 independent and the fusion inhibition experiments with SIVmac316 Env reported here were carried out in the absence of CD4.

In addition, minimalistic molecular mechanics and molecular modeling, which do not take into account the helical propensities of the C34 peptides, provides a semiquantitative correlation between calculated interaction free energies and observed IC_{50}s for two clusters of C34 peptides (namely, the LAV and N CM cluster, and the HIV-1 O CM, HIV-2 EHO and ALI, and SIV AGM cluster). The two clusters (Figure 4) correspond to C34 peptides with the lowest and highest helical propensities, respectively (Figure 5b,c).

We can therefore conclude that the inhibitory properties of C34 peptides can be rationalized on the basis of the strength of the interaction free energy between helical C34 and the N-terminal helical coiled-coil of gp41 and the helical propensity of the free C34 peptides.

Acknowledgment. This work was supported by the AIDS Targeted Anti-Viral program of the Office of the Director of the National Institutes of Health (to G.M.C. and C.A.B.). The AIDS Research and Reference Reagent Program, Division of AIDS, NIAID, NIH, is acknowledged for all recombinant vaccinia veruses and for the soluble CD4 employed in this study.

References

(1) Freed, E. O.; Martin, M. A. The role of human immunodeficiency virus type 1 envelope glycoproteins in virus infection. *J. Biol. Chem.* **1995**, *270*, 23883−23886.
(2) Moore, J. P.; Trkola, A.; Dragic, T. Co-receptors for HIV-1 entry. *Curr. Opin. Immunol.* **1997**, *7*, 551−562.
(3) Eckert, D. M.; Kim, P. S. Mechanisms of viral membrane fusion and its inhibition. *Annu. Rev. Biochem.* **2001**, *70*, 777−810.
(4) Furuta, R. A.; Wild, C. T.; Weng, Y.; Weiss, C. D. Capture of an early fusion-active conformation of HIV-1 gp41. *Nat. Struct. Biol.* **1998**, *5*, 276−279.
(5) Chan, D. C.; Kim, P. S. HIV entry and its inhibition. *Cell* **1998**, *93*, 681−684.
(6) Muñoz-Barroso, I.; Durell, S., Sakaguchi, K.; Appella, E.; Blumenthal, R. Dilation of the human immunodeficiency virus-1 envelope glycoprotein fusion pore revealed by the inhibitory action of a synthetic peptide from gp41. *J. Cell Biol.* **1998**, *140*, 315−323.
(7) Kliger, Y.; Gallo, S. A.; Peisajovich, S. G.; Muñoz-Barraso, I.; Avkin, S.; Blumenthal, R.; Shai, Y. Mode of action of an antiviral peptide from HIV-1: inhibition of a post-lipid mixing stage. *J. Biol. Chem.* **2001**, *276*, 1391−1397.
(8) Weissenhorn, W.; Dessen, A.; Harrison, S. C.; Skehel, J. J.; Wiley: D. C. Atomic structure of the ectodomain from HIV-1 gp41. *Nature* **1997**, *387*, 426−430.
(9) Chan, D. C.; Fass, D.; Berger, J. M.; Kim, P. S. Core structure of gp41 from the HIV envelope glycoprotein. *Cell* **1997**, *89*, 263−273.
(10) Tan, K.; Liu, J.; Wang, S.; Shen, S.; Lu, M. Atomic structure of a thermostable subdomain of HIV-1 gp41. *Proc. Natl. Acad. Sci. U.S.A.* **1997**, *94*, 12303−12308.
(11) Malashkevich, V. N.; Chan, D. C.; Chutkowski, C. T.; Kim, P. S. Crystal structure of the simian immunodeficiency virus (SIV) gp41 core: conserved helical interactions underlie broad inhibitory activity of gp41 peptides. *Proc. Natl. Acad. Sci. U.S.A.* **1998**, *95*, 9134−9139.
(12) Caffrey, M.; Cai, M.; Kaufmann, J.; Stahl, S. J.; Wingfield, P. T.; Covell, D. G.; Gronenborn, A. M.; Clore, G. M. Three-dimensional solution structure of the 44 kDa ectodomain of SIV gp41. *EMBO J.* **1988**, *17*, 4572−4584.
(13) Louis, J. M.; Nesheiwat, I.; Chang, L. C.; Clore, G. M.; Bewley, C. A. Covalent trimers of the internal N-terminal trimeric coiled-coil of gp41 and antibodies directed against them are potent inhibitors of HIV Envelope-mediated cell fusion. *J. Biol. Chem.* **2003**, *278*, 20278−20285.
(14) Wild, C. T.; Shugars, D. C.; Greenwell, T. K.; McDanal, C. B.; Matthews, T. J. Peptides corresponding to a predictive α-helical domain of human immunodeficiency virus type 1 gp41 are potent inhibitors of virus infection. *Proc. Natl. Acad. Sci. U.S.A.* **1994**, *91*, 9770−9774.
(15) Chan, D. C.; Chutkowski, C. T.; Kim, P. S. Evidence that a prominent cavity in the coiled-coil of HIV type 1 gp41 is an attractive drug target. *Proc. Natl. Acad. Sci. U.S.A.* **1998**, *95*, 15613−15618.
(16) Kliger, Y.; Shai, Y. Inhibition of HIV-1 entry before gp41-folds into its fusion-active conformation. *J. Mol. Biol.* **2000**, *295*, 163−168.
(17) Sia, S. K.; Kim, P. S. Protein grafting of an HIV-1 inhibiting epitope. *Proc. Natl. Acad. Sci. U.S.A.* **2003**, *100*, 9756−9761.
(18) Eckert, D. M.; Malashketevich, V. N.; Hong, L. H., Carr. P. A.; Kim, P. S. Inhibiting HIV-1 entry: discovery of D-peptide inhibitors that target the gp41 coiled-coil pocket. *Cell* **1999**, *99*, 103−115.
(19) Ferrer, M.; Kappor, T. M.; Strassmaier, T.; Weissenhorn, W.; Skehel, J. J.; Oprian, D.; Schreiber, S. L.; Wiley: D. C.; Harrison, S. C. Selection of gp41-mediated HIV-1 cell entry inhibitors from biased combinatorial libraries of nonnatural binding elements. *Nat. Struct. Biol.* **1999**, *6*, 953−960.
(20) Louis, J. M.; Bewley, C. A.; Clore, G. M. Design and properties of N_{CCG}-gp41, a chimeric gp41 molecule with nanomolar HIV fusion inhibitory activity. *J. Biol. Chem.* **2001**, *276*, 29485−29489.
(21) Root, M. J.; Kay, M. S.; Kim, P. S. Protein design of an HIV-1 entry inhibitor. *Science* **2001**, *291*, 884−888.
(22) Eckert, D. M.; Kim, P. S. Design of potent inhibitors of HIV-1 entry from the gp41 N-peptide region. *Proc. Natl. Acad. Sci. U.S.A.* **2001**, *98*, 11187−11192.
(23) Koshiba, T.; Chan, D. C. The prefusogenic intermediate of HIV-1 gp41 contains exposed C-peptide regions. *J. Biol. Chem.* **2003**, *278*, 7573−7579.
(24) Root, M. J.; Hamer, D. H. Targeting therapeutics to an exposed and conserved binding element of the HIV-1 fusion protein. *Proc. Natl. Acad. Sci. U.S.A.* **2003**, *100*, 5016−5021.
(25) Bewley, C. A.; Louis, J. M.; Ghirlando, R.; Clore, G. M. Design of a novel peptide inhibitor of HIV fusion that disrupts the internal trimeric coiled-coil of gp41. *J. Biol. Chem.* **2002**, *277*, 14238−14245.
(26) Lazzarin, A.; Clotet, B.; Cooper, D.; Reynes, J.; Arasteh, K.; Nelson, M.; Katlama, C.; Stellbrink, H. J.; Delfraissy, J. F.; Lange, J.; Huson, L.; DeMasi, R.; Wat, C.; Delehanty, J.; Drobnes, C.; Salgo, M. Efficacy of enfuvirtide in patients infected with drug-resistant HIV-1 in Europe and Australia. N. *Engl. J. Med.* **2003**, *348*, 2186−2195.
(27) Baldwin, C. E.; Sanders, R. W.; Deng, Y.; Jurriaans, S.; Lange, J. M.; Lu, M.; Berkhout, B. Emergence of a drug-dependent human immunodeficiency virus type 1 variant during therapy with the T20 fusion inhibitor. *J. Virol.* **2004**, *78*, 12428−12437.
(28) Greenberg, M. L.; Cammack, N. Resistance to enfuvirtide, the first HIV fusion inhibitor. *J. Antimicrob. Chemother.* **2004**, *54*, 333−340.
(29) Salzwedel, K.; Smith, E.; Dey, B.; Berger, E. A. Sequential CD4-receptor interactions in human immunodeficiency virus type 1 Env function: soluble CD4 activates Env for coreceptor-dependent fusion and reveals blocking activities of antibodies against cryptic conserved epitopes on gp120. *J. Virol.* **2000**, *74*, 326−333.
(30) Bohm, G.; Muhr, R.; Jaenicke, R. Quantitative analysis of protein far UV circular dichroism spectra by neural networks. *Prot. Eng.* **1992**, *5*, 191−195.
(31) Feng, Y.; Broder, C. C.; Kennedy, P. E.; Berger, E. A. HIV-1 entry cofactor: functional cDNA cloning of a seven-transmembrane, G protein-coupled receptor. *Science* **1996**, *272*, 872−877.
(32) Broder, C. C., Berger, E. A. Fusogenic selectivity of the envelope glycoprotein is a major determinant of human immunodeficiency virus type 1 tropism for $CD4^+$ T-cell lines versus primary macrophages. *Proc. Natl. Acad. Sci. U.S.A.* **1995**, *92*, 9004−9008.
(33) Dimitrov, D. S., Norwood, D.; Stantchev, R. S., Feng, Y.; Xiao, S.; Broder, C. C. A mechanism of resistance to HIV-1 entry: inefficient interactions of CXCR4 with CD4 and gp120 in macrophages. *Virology* **1999**, *259*, 1−6.
(34) Doranz, B. J.; Rucker, J.; Yi, Y.; Smyth, R. J.; Samson, M.; Peiper, S. C.; Parmentier, M.; Collman, R. G.; Doms, R. W. A

dual-tropic primary HIV-1 isolate that uses fusin and the β-chemokine receptors CKR-5, CKR-3 and CKR-2b as fusion cofactors. Cell **1996**, *85*, 1149−1158.
(35) Edinger, A. L.; Makowski, J. L.; Doranz, B. J.; Margulies, B. J.; Lee, B.; Rucker, J.; Sharron, M.; Hoffman, T. L.; Berson, J. F.; Zink, M. C.; Hirsch, V. M.; Clements, J. E.; Doms, R. W. CD4-indepedent, CR5-dependent infection of brain capillary endothelial cells by a neurovirulent simian immunodeficiency virus strain. *Proc. Natl. Acad. Sc. U.S.A.* **1997**, *94*, 14742−14747.
(36) Wang, J.; Cieplak, P.; Kollman, P. A. How well does a restrained electrostatic potential (RESP) model perform in calculating conformational energies of organic and biological molecules? *J. Comput. Chem.* **2000**, *21*, 1049−1074.
(37) Onufriev, A.; Bashford, D.; Case, D. A. Exploring protein native states and large-scale conformational changes with a modified generalized Born model. *Proteins* **2004**, *55*, 383−394.
(38) Weiser, J.; Shenkin, P. S.; Still, W. C. Approximate Atomic Surfaces from Linear Combinations of Pairwise Overlaps (LCPO). *J. Comput. Chem.* **1999**, *20*, 217−230.
(39) Canutescu, A. A.; Shelenkov, A. A.; Dunbrack, R. L., Jr. A Graph Theory Algorithm for Protein Side-Chain Prediction. *Protein Sci.* **2003**, *12*, 2001−2014.
(40) Thompson, J. D.; Gibson, T. J.; Plewniak, F.; Jeanmougin, F.; Higgins, D. G. The ClustalX windows interface. flexible strategies for multiple sequence alignment aided by quality analysis tools. *Nucleic Acids Res.* **1997**, *24*, 4876−4882.
(41) Buck, M. Trifluoroethanol and colleagues: cosolvents come of age: recent studies with peptides and proteins. *Q. Rev. Biophys.* **1998**, *31*, 297−335.
(42) Muñoz, V.; Serrano, L. Elucidating the folding problem of helical peptides using empirical parameters. *Nat. Struct. Biol.* **1994**, *1*, 399−409.
(43) Judice, J. K.; Tom, J. Y. K.; Huang, W.; Wrin, T.; Vennari, J.; Petropoulos, C. J.; McDowell, R. S. Inhibition of HIV type 1 infectivity by constrained α-helical peptides: implications for the viral fusion mechanism. *Proc. Natl. Acad. Sci. U.S.A.* **1997**, *94*, 13426−13430.
(44) Gallo, S. A.; Sackett, K.; Rawat, S. S.; Shai, Y.; Blumenthal, R. The stability of the intact envelope glycoproteins is a major determinant of sensitivity of HIV/SIV to peptidic fusion inhibitors. *J. Mol. Biol.* **2004**, *340*, 9−14.

JM049026H